



Article

Next-Generation Lubricity in Deep Drawing: The Synergistic Benefits of PIL and Talc on Water-Based Lubricants

Victor Velho de Castro ^{1,*}, Cristiano Ev ¹, Leandro Câmara Noronha ¹, Matheus Bullmann ¹, Louise Etcheverry ¹, Leonardo Moreira dos Santos ², Rafael Marquette Vargas ³, Silvana Mattedi ⁴, Roberto Moreira Schroeder ¹  and Célia de Fraga Malfatti ¹ 

¹ Corrosion Research Laboratory (LAPEC), Department of Metallurgy, Federal University of Rio Grande do Sul (UFRGS), Porto Alegre 91509-900, RS, Brazil; matheus.bullmann@ufrgs.br (M.B.); louise.etccheverry@am.senai.br (L.E.)

² School of Technology, Pontifical Catholic University of Rio Grande do Sul (PUCRS), Porto Alegre 90619-900, RS, Brazil

³ Federal Institute of Education, Science and Technology Sul-Riograndense, Charqueadas 96745-000, RS, Brazil

⁴ Applied Thermodynamics Laboratory, Department of Chemical Engineering, Federal University of Bahia (UFBA), Salvador 40210-630, BA, Brazil

* Correspondence: victor.castro@ufrgs.br; Tel.: +55-51-98488-5691

Abstract: This study aims to assess the effectiveness of water-based formulations featuring m-2HEAOL and talc particles in deep drawing applications. The coefficient of friction (COF) was measured through bending under tension (BUT) tests, while the interaction mechanism between protic ionic liquid (PIL) and talc particles was analysed using FTIR, XPS, and TGA analyses. The results indicate that the formulation containing 8 wt% PIL and 0.5 wt% talc exhibited the best lubricating performance. This was due to the interaction of the PIL oleate molecules with the Mg found in the talc basal layer, which enhanced the cleavage capacity of this mineral, ultimately improving the lubricity of the formulation.

Keywords: protic ionic liquid; talc; bending under tension; steel



Citation: de Castro, V.V.; Ev, C.; Noronha, L.C.; Bullmann, M.; Etcheverry, L.; dos Santos, L.M.; Vargas, R.M.; Mattedi, S.; Schroeder, R.M.; Malfatti, C.d.F.

Next-Generation Lubricity in Deep Drawing: The Synergistic Benefits of PIL and Talc on Water-Based Lubricants. *Metals* **2024**, *14*, 705. <https://doi.org/10.3390/met14060705>

Academic Editor: Slobodan Mitrovic

Received: 16 May 2024

Revised: 3 June 2024

Accepted: 10 June 2024

Published: 14 June 2024



Copyright: © 2024 by the authors. Licensee MDPI, Basel, Switzerland. This article is an open access article distributed under the terms and conditions of the Creative Commons Attribution (CC BY) license (<https://creativecommons.org/licenses/by/4.0/>).

1. Introduction

If not well managed, tribological phenomena in sheet-metal-forming processes can lead to unfavourable outcomes, such as changes in force and energy parameters [1]. These phenomena can also cause a premature reduction in tool life and defects in stamped parts [2]. Controlling friction resistance is essential, as it influences the material flow in the tool and the surface finish of produced parts [3].

The bending under tension (BUT) test is the most widely used procedure to simulate and isolate the friction generated in a stamping process. In this test, a force is applied to one end of the sample to cause movement relative to the bending pin. At the other end of the sample, a force opposite to the movement is applied when subjecting it to the effect of stretching [4]. The test is designed for studying the influence of parameters on friction and limits of lubrication, simulating stamping operations [5]. Numerous studies have investigated this subject and obtained the value of friction as a result.

In their study, Moghadam et al. [6] employed the acoustic emission measurement technique to monitor friction conditions during the BUT test. The results showed that this accurately assessed lubrication limits and described friction conditions during well formation. In another research, a combination of 2D and 3D models of the tensile bending test with thermal and thermomechanical procedures in steady and transient states was used. The methodology proposed by the authors effectively and accurately predicted the interface temperature in the test tool under specific conditions [7].

Folle and Schaeffer [8] devised a new methodology and equation for measuring the coefficient of friction (COF) in BUT tests. Their study revealed that previously developed equations fail to accurately predict friction at the sheet interface. Consequently, the researchers created a simpler-to-apply equation that provides satisfactory results.

The increasing demand for environmentally friendly production methods has resulted in a transition from conventional lubricants used in mechanical forming operations to water-based lubricants [9]. To optimize the performance of these lubricants, top-quality additives are used, including surface/interface active molecules [10].

Currently, there is a search by several researchers to develop environmentally friendly lubricants. Polajnar et al. [11] investigated the lubricity of four base oils with different chemical structures (paraffinic, naphthenic, and water) for application in steel stamping. Low-viscosity naphthenic oil performs very similarly to high-viscosity oils, and can reduce friction and wear.

In their recent review article, Aiman et al. [12] discussed recent research that proposed the application of biolubricants based on vegetable and animal oil to replace mineral oils. According to the results of these studies, the properties of the fatty acids present in these lubricants guarantee good lubrication in mechanical forming manufacturing. Furthermore, they highlighted that there is a better affinity on the surface of the metal where the unsaturated fatty acid is present. However, all of these studies are still in the experimental phase.

Castor and sesame oils are examples of studied vegetable oils. Tests carried out on a ball-on-disc tribometer under boundary lubrication conditions demonstrate performance similar to mineral oils [13].

Combinations of natural and ecological materials such as boric acid (H_3BO_3) and edible vegetable oils [14] are also being studied in mechanical forming operations. It was found that pure palm oil and the formulation with the addition of 5% by weight of H_3BO_3 was the most effective in reducing the coefficient of friction. Furthermore, the authors highlight that the addition of boric acid can increase lubrication efficiency by up to 15%.

In addition to oils of vegetable origin, solid nanoparticles and ionic liquids are examples of environmentally friendly additives that improve tribological properties, reducing friction, wear, and corrosion [15].

Among the different types of ionic liquids, protic ionic liquids (PILs) have shown promise as a good lubricant due to their high viscosity and low volatility. PILs are also effective solvents and can be used as additives to reduce friction in various contacts [16]. Several researchers have proposed PILs as potential lubricant additives [17–19]. Gussain et al. [20] used ionic liquids synthesized from fatty acids as additives to a polyol ester lubricant base oil, which demonstrated a substantial improvement in friction reduction (28–60%) and anti-wear (20–28%) properties under the lubrication regime limit. Furthermore, the addition of 2% fatty acid ionic liquid to polyol ester, composed of fatty acid, proved to be non-corrosive.

To optimize the lubricity of water-based lubricants, many manufacturers have incorporated graphite particles [21,22]. However, this addition has caused galvanic corrosion when in contact with steel in aqueous solutions due to graphite's noble electrochemical potential, which increases cathodic reactions and leads to equipment and component corrosion. Therefore, using solid lubricants such as talc instead of graphite is a viable and cost-effective option for water-based lubricants.

Our research group has previously found that PIL m-2HEAOL is an effective lubricant in its pure state [23] and in water-based formulations with talc and bentonite lubricating particles [24,25]. PIL m-2HEAOL also improves corrosion inhibition [26–28] and has low toxicity [29]. Despite these positive attributes, this molecule has yet to undergo testing for mechanical forming applications such as stamping.

The main objective of this work is to evaluate the effectiveness of water-based formulations that contain m-2HEAOL and talc particles in deep drawing applications. The COF was determined using BUT tests, while FTIR, XPS, and TGA analyses were used to

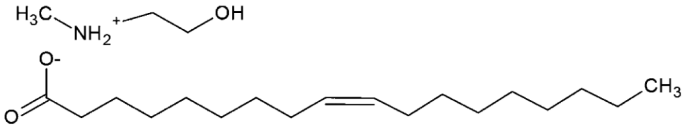
determine the interaction mechanism between PIL and talc particles. The performance of formulations with PIL was compared to those containing a commercial additive as a reference.

2. Materials and Methods

2.1. Characterization of Lubricants

This research evaluates the effectiveness of lubricants containing deionized water, lubricating particles, and PIL (m-2HEAOL—Table 1) for deep drawing applications. The m-2HEAOL was synthesized by the research group at the Federal University of Bahia (UFBA). The characterization of the PIL was carried out and presented in a previously published paper [23]. The performance of these lubricants was compared to a commercial water-soluble lubricant that was used as an additive. The commercial lubricant is characterized by being non-corrosive and odourless hybrid synthetic release agent, without the addition of petroleum jelly, mineral, or vegetable oils. It is applied in lubrication in metal forming, casting, and die-casting. It is characterized by forming a friction-reducing film. To determine the optimal proportion of PIL and commercial additive, tests were conducted using 1 wt%, 3 wt%, and 8 wt% of each. Schumacher brand talc particles were also included in the formulations at a concentration of 0.5 wt%, which is consistent with previous studies [30]. Notably, the concentration of 8% by weight is close to the solubility limit of m-2HEAOL in water. After incorporating the particles, the lubricants were allowed to settle for 24 h. Before conducting wear and corrosion tests, the dispersions were mechanically agitated for 30 min.

Table 1. PIL used as an additive in the investigated lubricants. Adapted from Vega et al. [23].

PIL	Structure
m-2HEAOL N-methyl-2-hydroxyethylammonium oleate	

The formulation nomenclatures are presented in Table 2. Each component of the formulation, except the deionized water, is referred to by the term “additive”. The pH of the formulations presented values close to 8.0.

Table 2. Composition of the formulations.

Lubricant Nomenclature	Composition (% by Weight)
m-2HEAOL_1%_WP	H ₂ O + 1 wt% m-2HEAOL
m-2HEAOL_3%_WP	H ₂ O + 3 wt% m-2HEAOL
m-2HEAOL_8%_WP	H ₂ O + 8 wt% m-2HEAOL
m-2HEAOL_1%_TC_0.5%	H ₂ O + 1 wt% m-2HEAOL + 0.5 wt% Talc
m-2HEAOL_3%_TC_0.5%	H ₂ O + 3 wt% m-2HEAOL 0.5 wt% Talc
m-2HEAOL_8%_TC_0.5%	H ₂ O + 8 wt% m-2HEAOL 0.5 wt% Talc
* Commercial_1%_WP	H ₂ O + 1 wt% commercial additive *
* Commercial_3%_WP	H ₂ O + 3 wt% commercial additive *
* Commercial_8%_WP	H ₂ O + 8 wt% commercial additive *
* Commercial_1%_TC_0.5%	H ₂ O + 1 wt% commercial additive * + 0.5 wt% Talc
* Commercial_3%_TC_0.5%	H ₂ O + 3 wt% commercial additive * + 0.5 wt% Talc
* Commercial_8%_TC_0.5%	H ₂ O + 8 wt% commercial additive * + 0.5 wt% Talc

* Water-soluble commercial lubricant.

The rheological properties of the formulations were examined using an Ar 1500 ex rheometer, which applied shear rates ranging from 0 to 1000 s⁻¹ at a constant temperature of 23 °C for 2 min. The tests were conducted according to the guidelines of DIN 545012.001.

2.2. Manufacturing and Characterization of Steel Samples

SAE 1050 steel pins samples were machined with 50 mm length and 24 mm diameter. The pins were surface quenched, and were tempered at 400 °C. Afterwards, the cylindrical grinding process was applied to the pins' surfaces. SAE 1010 steel plates samples measuring 21 mm wide and 1300 mm long were polished with silicon carbide sandpaper (#100). These materials are employed in a variety of stamping functions.

To determine the chemical composition of the samples, a Bruker emission spectrometer (OES) of the model Q2 ION was used. The microhardness was measured using a Mitutoyo microhardness meter, model HV-100, with a 50 g load. The microstructures were evaluated using a Zeiss optical microscope, model Axio Lab.A1, after conditioning with 3 wt% Nital. An image analysis was performed with the ZEN 2.6 software (blue edition).

To measure the average surface roughness (Ra and Rz), we used the Mitutoyo linear rugosimeter, model SJ-400. The samples underwent a thorough cleaning process, including using water and neutral detergent, followed by ultrasound cleaning with acetone, which in turn was followed by cleaning using ethyl alcohol and deionized water, for 15 min each, and then they were finally dried with a portable air device.

2.3. Bending under Tension (BUT) Test

BUT tests were conducted to evaluate the lubricity of the proposed formulations in the stamping operations. The equipment we used was developed at the Corrosion Research Laboratory (LAPEC) of the Federal University of Rio Grande do Sul (UFRGS). It is computationally controlled and coupled to an universal traction machine (Intermetric, model 4156 ESP). The lubricants were applied to the plates and pins by brushing, and we applied a counter tension force of 843 N (86 kgf). We performed tests in triplicate for each condition, calculating the COF during the test (sliding distance of 200 mm). The COF was calculated using the equation proposed by Folle and Schaeffer [8]:

$$\text{COF} = \frac{4T}{\pi R(F_1 + F_2)}$$

where:

T represents the torque on the pin, R is the radius of the pin, F_1 is the actuation force, and F_2 is the counter tension force.

2.4. Characterization of Talc Particles

The talc particles used in the formulations proposed on Table 2 were analysed. To separate the emulsion particles, the formulations were centrifuged at 2000 RPM for 30 min. The talc particles were removed from the PIL formulations, and the samples were shaken in deionized water and centrifuged three times.

TA instruments equipment, model SDT Q600, was used for thermogravimetric analysis (TGA) with N₂ 5.0 gas (flow rate of 100 mL/min) up to a temperature of 800 °C and platinum pans.

Fourier Transform Infrared Spectroscopy (FTIR) measurements were conducted at 25 °C using a Bruker Vertex 70 V spectrometer and the KBr tablet method.

X-ray photoelectron spectroscopy (XPS) was performed with Omicron-SPHERA analysers using an Al-K α X-ray source ($h\nu = 1486.7$ eV). The measurements were conducted in the long scan, and C 1s, O 1s, Si 2p, and Mg 2p electronic regions. The spectra were calibrated using the peak of the Si 2p region at 103.5 eV. The Casa XPS software version 2.3.15, with a Shirley-type background was used to analyse the XPS spectra.

3. Results

3.1. Characterization

Table 3 presents the chemical composition, hardness, and roughness, Ra and R_z. The percentage of alloy elements in both the pin (SAE 1050) and the plate (SAE 1010) met

the specifications for their respective materials. After surface heat treatment, the pins displayed a homogenous, tempered martensitic structure on the surface, while the core exhibited a primarily pearlitic microstructure (Figure 1A,B). As a result, the material's surface hardness was measured to be approximately 550 HV (52 HRC). The sheets' microstructure (Figure 1C,D) consisted mostly of a ferritic matrix with pearlite islands at the grain boundary. The micrograph of the longitudinal sample position (Figure 1D) showed elongated grains, likely due to the manufacturer's cold rolling process. Therefore, the surface hardness of the material was about 128 HV (71 HRB).

Table 3. Chemical composition, hardness, and roughness of the steel samples.

Steel	Fe (%)	C (%)	Si (%)	Mn (%)	P (%)	S (%)	Hardness (HV)	R _a (μm)	R _z (μm)
SAE 1010	Balance	0.10	0.10	0.40	0.02	0.01	128 (±23)	0.24 (±0.03)	4.63 (±0.53)
SAE 1050	Balance	0.51	0.18	0.76	0.01	0.01	550 (±50)	0.132 (±0.01)	1.49 (±0.14)

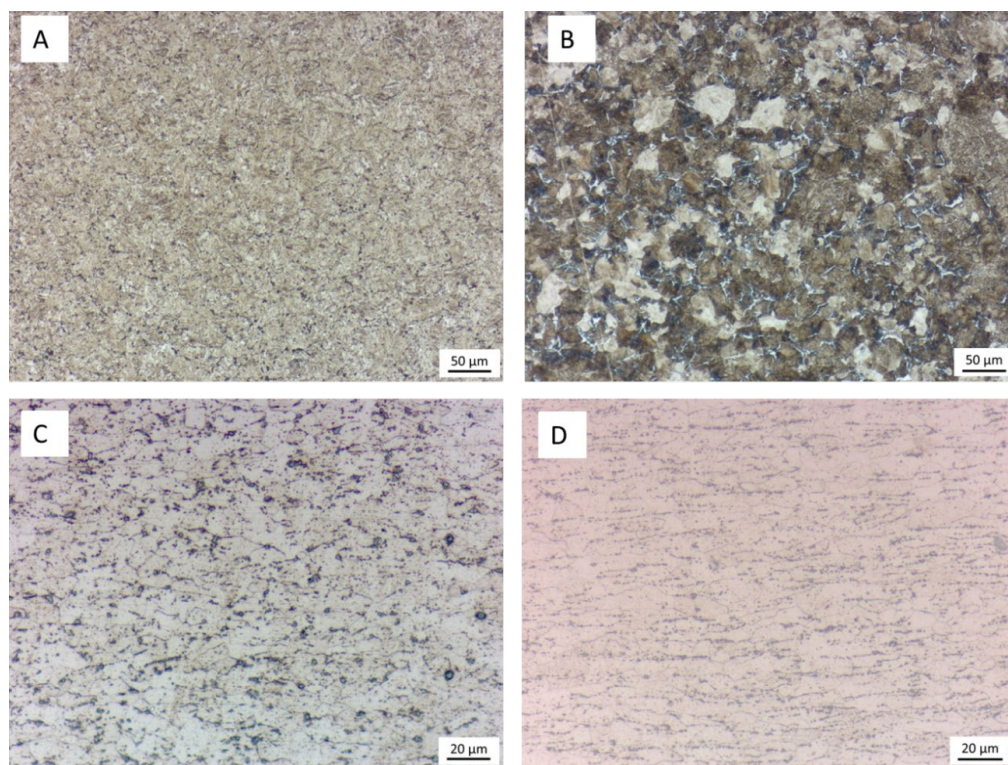


Figure 1. Micrographs of the samples used in the study. Attack: Nital. (A): Pin surface; (B): centre of the pin; (C): cross-section of the plate; (D): longitudinal section of the sheet.

Cylindrical grinding of the pins yielded a surface roughness R_a and R_z of 0.132 μm and 1.49 μm, respectively. The surface preparation process also produced a roughness R_a of 0.132 μm and R_z of 4.63 μm.

The current study utilized talc particles that our research group had previously analysed for their particle size distribution, morphology, and phases [24]. The average particle diameter was determined to be approximately 29.6 μm. Particles larger than 0.5 μm tend to precipitate and create unstable suspensions [31]. Talc has a known lubrication capacity generated by its layered structure linked by Van der Waals bonds that move easily [32], in addition to the lamellar shape observed in these particles, which can also contribute to increased lubricity [24,33].

3.2. Rheological Behaviour of Particle-Free Formulations

Moving onto the rheological behaviour of particle-free formulations, Figure 2 shows that the formulations exhibit non-Newtonian behaviour, specifically pseudo-plasticity [34], which is characterized by decreasing viscosity with increasing applied tension [35]. This viscosity behaviour is caused by the solvation of polar solute molecules and solvents, which increases viscosity at rest, but decreases it with increasing applied tension as the shear action destroys the solvated layers. Recent research suggests that lubricants with Newtonian behaviour may not meet the demands of newer technological applications, such as those in wire drawing [36]. Arif et al. [37] demonstrated that pseudo-plastic lubricants can reduce the friction coefficient in high-pressure systems like bearings.

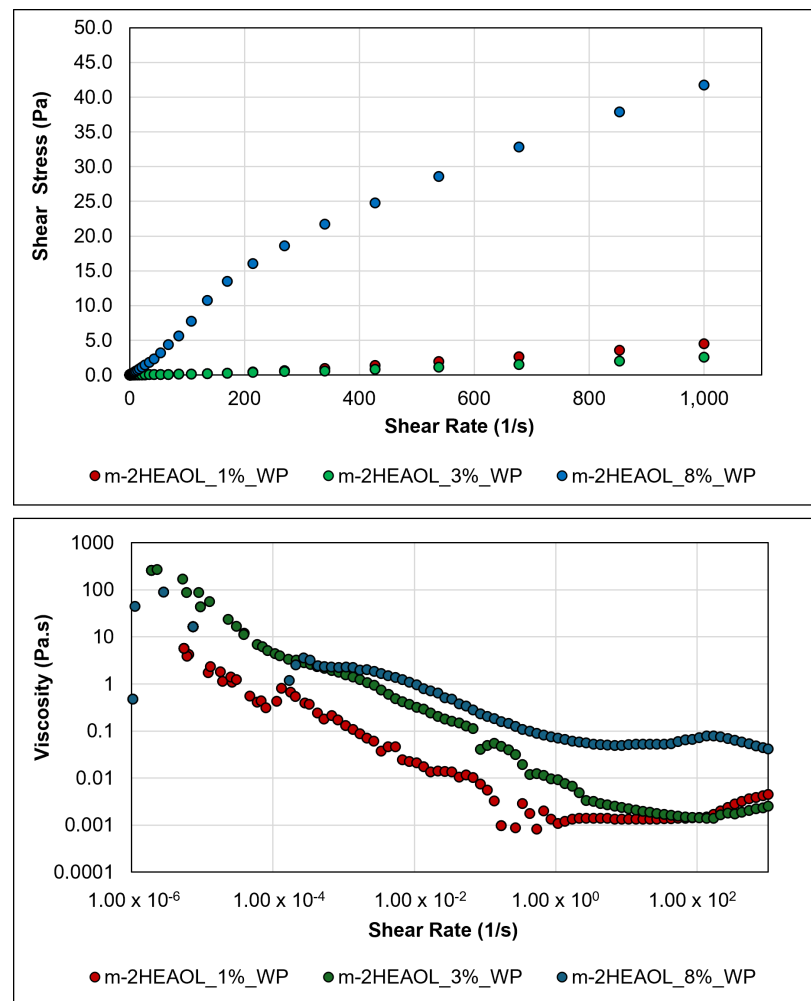


Figure 2. Rheological behaviour of the studied lubricant fluids.

Although these formulations present similar rheological behaviour, it is noted that the formulation containing 8 wt% PIL maintains viscosity at higher values than the other formulations at a shear rate of up to two orders of magnitude between 10^0 s^{-1} and 10^2 s^{-1} , presenting values close to 0.01 Pa.s until the end of the test.

3.3. Bending under Tension Test

3.3.1. Formulations with Commercial Additives

Figures 3 and 4 show the friction coefficients obtained in BUT tests for the formulations presented in Table 2. Tests were conducted for the formulations containing commercial additives, and formulations containing PIL (item b) were used for comparative purposes. Formulations without talc particles showed similar behaviour. The COF values were

close to 0.08 after 300 s of testing in all three studied concentrations. This result suggests that small percentages of commercial lubricant in an aqueous medium can achieve the maximum possible lubrication capacity, and increasing the amount of lubricant in the mixture does not necessarily result in better lubrication.

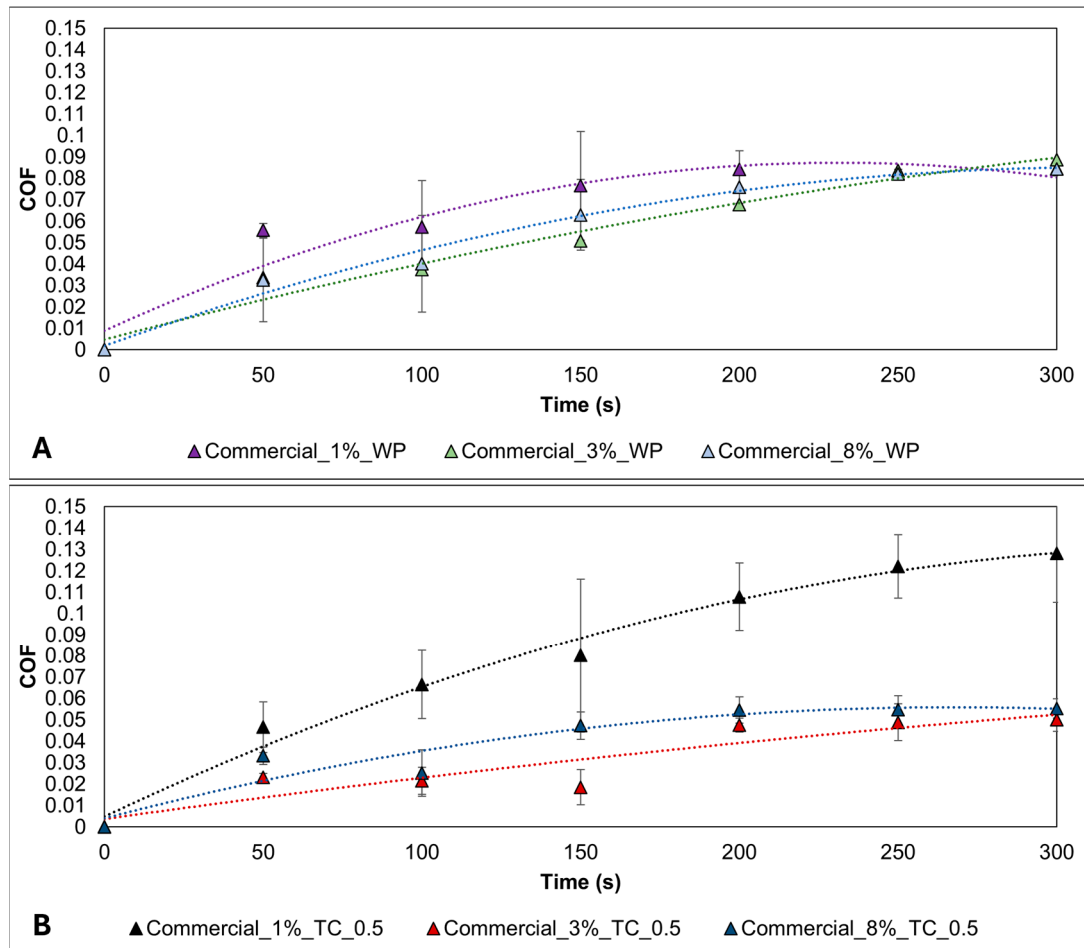


Figure 3. Friction coefficients obtained from BUT tests. (A): Formulations with commercial additives without talc particles; (B): Formulations with commercial additives and talc particles.

The addition of talc particles (Figure 3B) changed the lubricity of the formulations containing commercial additives. In formulations containing 3 wt% and 8 wt% commercial additive, the COF was reduced to values close to 0.04, a 50% reduction resulting from the action of these particles. This indicates a synergistic effect between the commercial lubricant and the talc particles at concentrations of 3 wt% and 8 wt% in this lubricant. These results confirm a previous study by our research group, where talc particles added to similar formulations were able to reduce the worn volume in tribometer tests carried out in a ball-on-plate configuration [24].

For the Commercial_1%_TC_0.5 formulation, the COF value rose close to 0.12. This suggests that the addition of talc particles reduced the lubricity compared to the Commercial_1%_WP formulation, which does not contain talc particles. It is possible that the known lubricant adsorption/absorption capacity of talc [38,39] reduced the concentration of commercial additive available in the aqueous solution, leading to a decrease in the lubricity of this formulation.

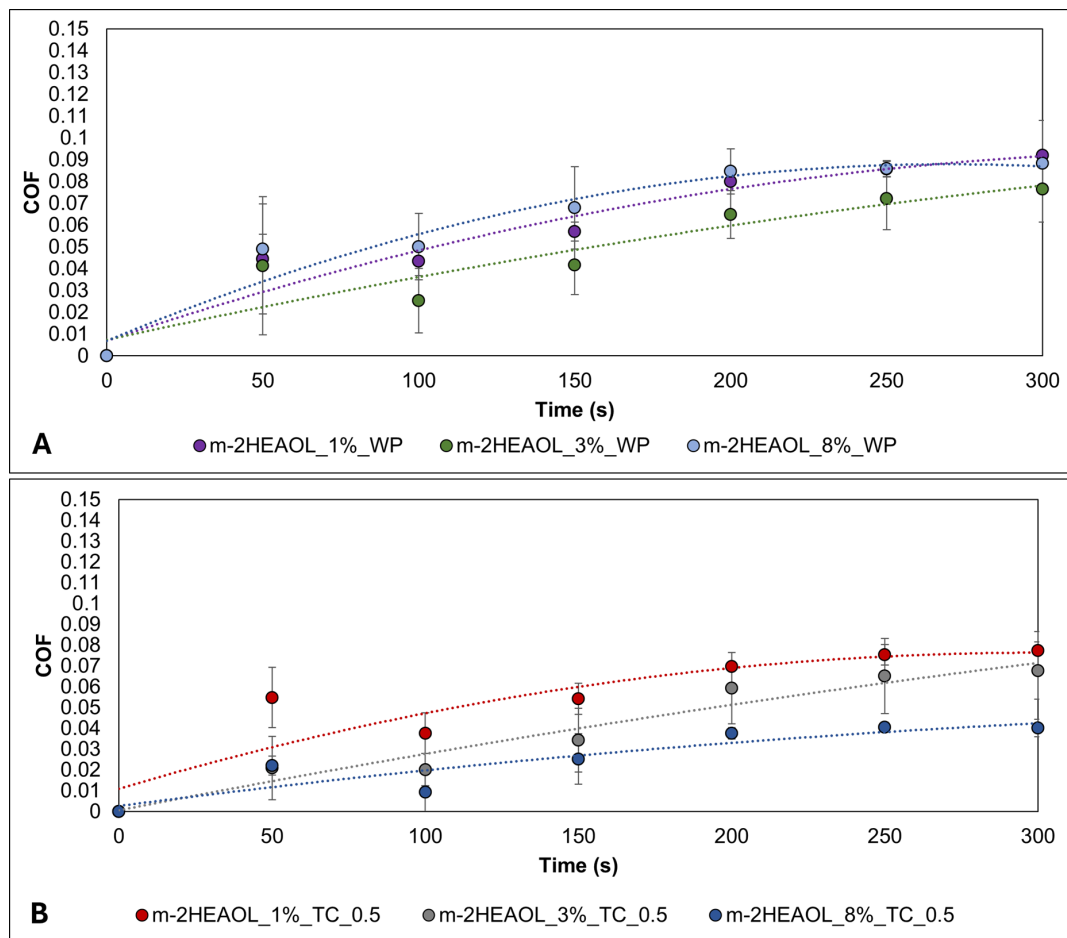


Figure 4. Friction coefficients obtained from BUT tests. (A): Formulations with m-2HEAOL without talc particles; (B): Formulations with m-2HEAOL and talc particles.

3.3.2. Formulations with m-2HEAOL Lubricant

After 300 s of testing, it was discovered that formulations containing m-2HEAOL without added particles (Figure 4A) exhibited comparable COF values to those containing commercial additives (COF value close to 0.08). This suggests that using m-2HEAOL as a lubricant additive could be a viable alternative to current market products.

When comparing the friction coefficients of the tests of the formulations with PIL (Figure 4B), in the formulations with 1 wt% and 3 wt%, it is clear that adding 0.5 wt% of talc particles did not change the COF. This implies that the dominant factor in the COF values obtained from these tests was the lubricity provided by the adsorption/absorption of m-2HEAOL on the metal surfaces of the plate and pin [24,25].

The addition of 1 wt% PIL and 0.5 wt% talc did not increase the COF, unlike what was observed in the commercial lubricant. This suggests a difference in the mechanism of action of PIL in comparison to the commercial additive. However, the m-2HEAOL_8%_TC_0.5 formulation displayed the lowest average COF value, approximately 0.035, after 300 s of testing.

It was observed that the 8 wt% formulation had a higher viscosity compared to other formulations (Figure 2). However, this increase in viscosity was not the sole reason for the increase in lubricity of the m-2HEAOL_8%_TC_0.5% formulation. This was evident from the fact that there was no significant difference in the friction coefficients measured in the three formulations with PIL and without talc particles. It is possible that the lubricity of this formulation was enhanced due to the interactions between PIL and talc particles.

Due to the standardization of the surface roughness and hardness of the samples of both steels used in the BUT test, only the properties of the lubricants were significant in the COF differences detected.

3.4. Analysis of the Talc–PIL Interaction

Various tests were conducted to study the interaction between talc particles and m-2HEAOL molecules. The particles were added to formulations and removed after 24 h, as described in item 2 of the Materials and Methods Section. The particles were named m_1%, m_3% and m_8%, and were each included in formulations containing 1 wt%, 3 wt%, and 8 wt% PIL, respectively.

3.4.1. FTIR Analysis

Figure 5D shows the FTIR spectra for m-2HEAOL. The broadband between 3580 cm^{-1} and 3250 cm^{-1} is related to the stretching (ν) of the O–H (hydroxyl) with hydrogen bonding. At approximately 1714 cm^{-1} , the typical peak of C=O carbonyl bonds stretches (ν) is observed. The characteristic symmetric and asymmetric stretching of the C–H bonds of alkanes was detected between 2960 cm^{-1} and 2850 cm^{-1} [40]. At 1560 cm^{-1} and 1629 cm^{-1} , there are vibrations related to N–H bending, which are associated with the positively charged part of the ionic liquid. Furthermore, the peak at 1260 cm^{-1} is possibly associated with the C–N bond, which is related to the hydroxyethylammonium molecule [28].

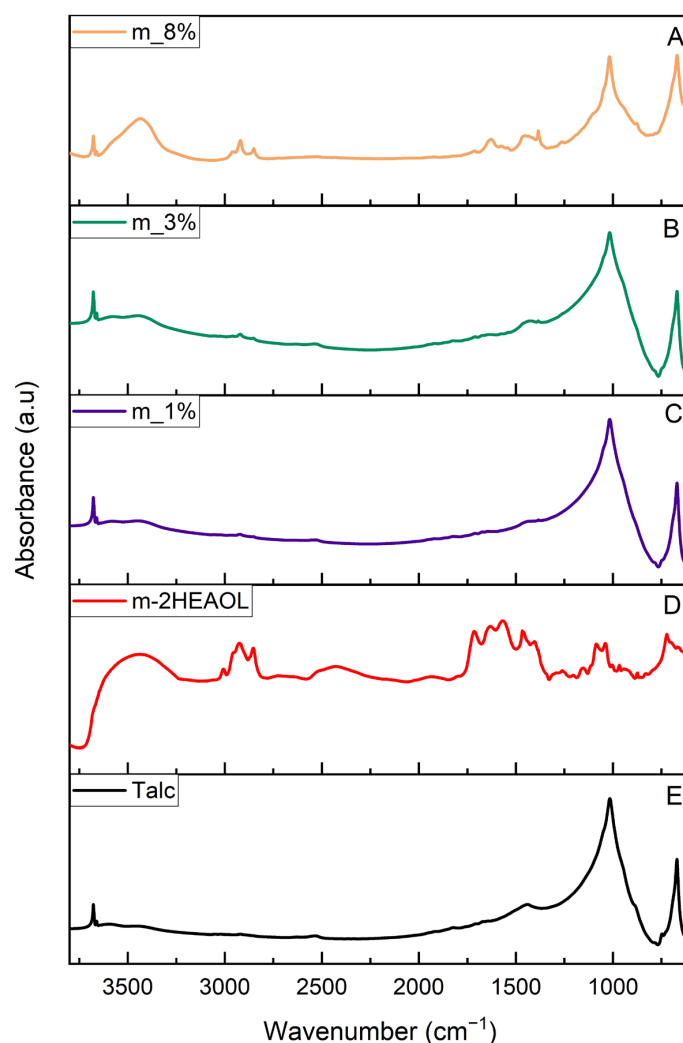


Figure 5. FTIR spectra of: m-2HEAOL (A), m_8% talc; (B) m_3% talc; (C) m_1% talc; (D) m-2HEAOL; (E) untreated talc.

In Figure 5E, a typical pattern of talc is observed. Characteristic peaks of Mg_3OH appear in 3677 cm^{-1} and 670 cm^{-1} . A weak band in 3660 cm^{-1} due to $Mg_2Fe^{II}OH$ can indicate a trace of FeII contamination in octahedral talc sheets. The sharp peak in approximately 1016 cm^{-1} was related to Si-O stretching [41,42].

The IR spectra of samples of talc m_1% and m_3% (Figure 5C,D) shows the typical pattern of untreated talc and characteristic peaks of organic groups with weak intensity, such as O-H, C-H, and C=O. This can indicate a partial interaction between ionic liquid and talc in minor percentages of the mixture. However, more pronounced changes were observed in the m_8% talc (Figure 5A). This spectrum shows all the main peaks of untreated talc and ionic liquid (described previously) with high intensity. At this mixing percentage, m-2HEAOL can interact with talc crystallographic planes, forming bonds.

3.4.2. XPS Analysis

X-ray photoelectron spectroscopy (XPS) measurements were used to examine the chemical states and compositions of talc samples with different concentrations: m_1%, m_3%, and m_8% (Figure 6). The samples contained carbon (C), oxygen (O), magnesium (Mg), and silicon.

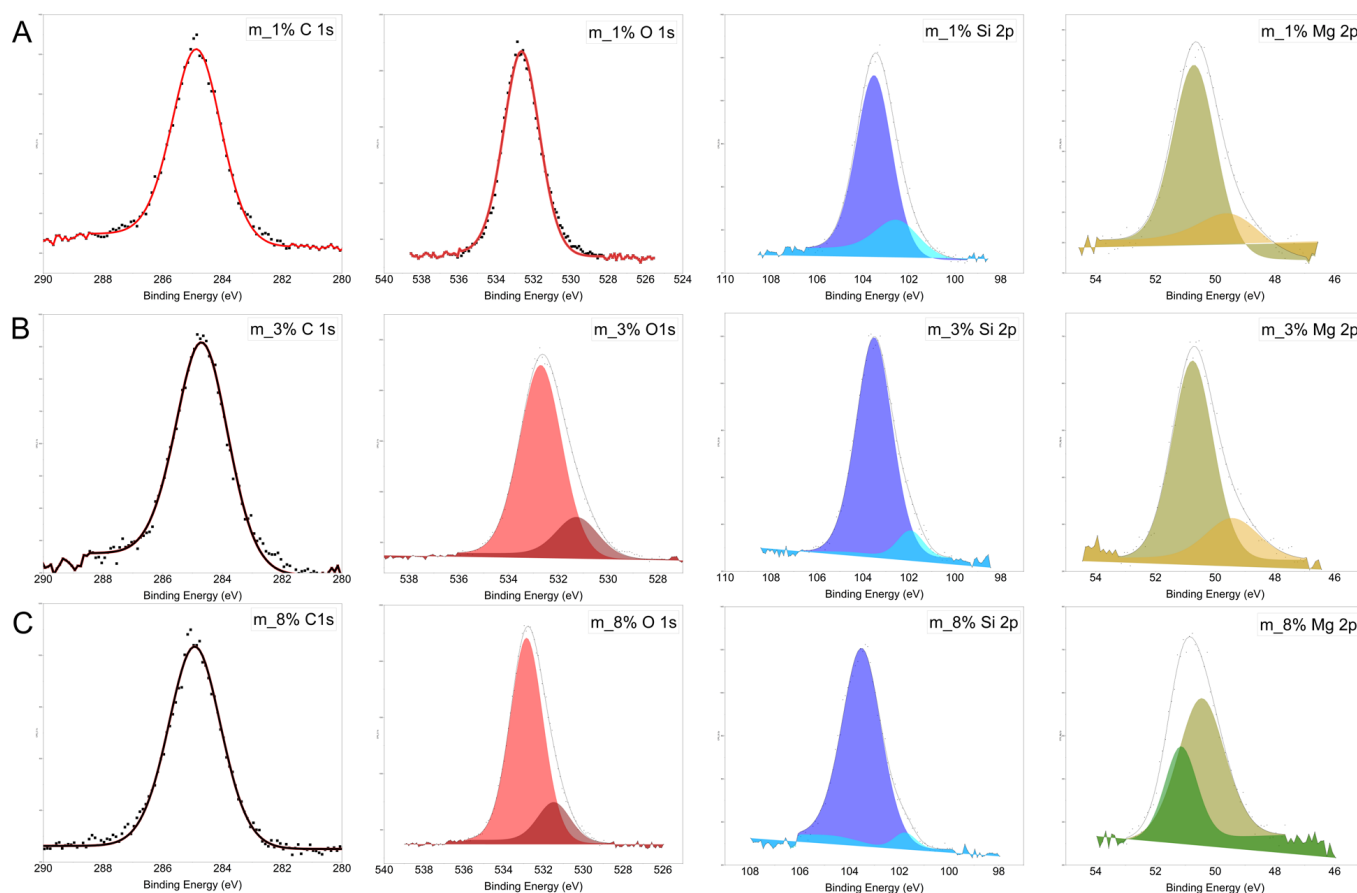


Figure 6. XPS analysis. (A): m_1% talc sample; (B): m_3% talc sample; (C): m_8% talc sample.

The core-level XPS spectra for C 1s, O 1s, Si 2p, and Mg 2p were analysed. The high-resolution XPS spectra of the O 1s for all samples showed a peak at $\sim 532.8\text{ eV}$ related to the Si-O bond. In addition, for the m_8% sample, another component was observed at 531.7 eV related to the Mg-O bond [43]. This indicates that when talc is added to an 8 wt% m-2HEAOL formulation, a bond is formed between the talc and the ionic liquid.

In the high-resolution spectrum of the Si 2p region, a component related to silicon oxide was observed at 103.5 eV for all samples. This bond is formed by the tetrahedron-layered talc structure. At 131.9 eV , a component related to the Si-C bond was also observed [44].

When analysing the high-resolution spectrum of Mg 2p, two components related to metallic Mg and in the 2+ oxidation state were observed for samples of m_1% and m_3% at 49.6 and 50.6 eV. Both components are related to the brucite structure (basal plane). For the m_8% sample, a component related to the 2+ oxidation state and another component at ~51.1 eV related to the Mg-O bond were observed [45]. This result is consistent with the results obtained in FTIR, which indicate that the bonding of talc with the ionic liquid occurs through the bonding of magnesium with a hydroxyl of the ionic liquid.

3.4.3. TGA Analysis

To determine the amount of PIL adsorbed, TGA analyses were conducted on the talc particles (Figure 7). The particles that were not used in the formulations and were only used as a reference showed almost zero mass loss. This is because talc is known for its thermal stability in the temperature range evaluated [46].

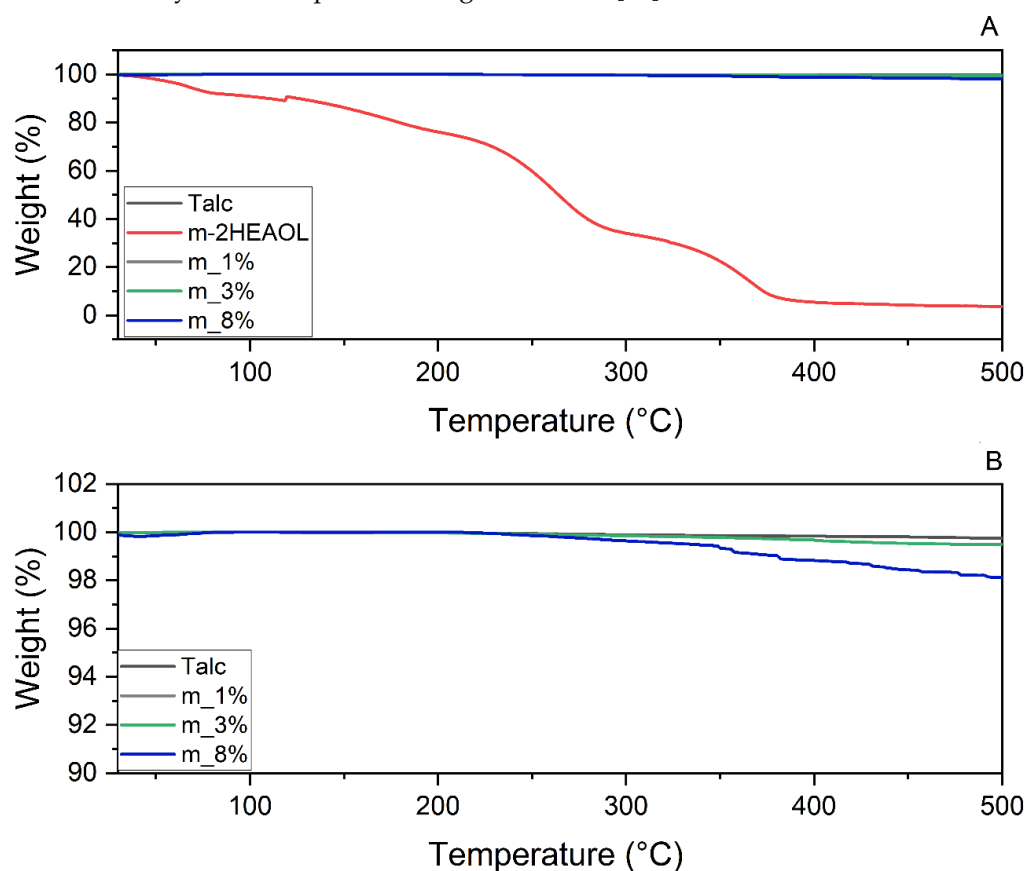


Figure 7. (A): TGA analysis of talc particles and m-2HEAOL. (B): TGA analysis of talc particles with expanded scale of mass loss between 90% and 100%.

The thermal degradation of m-2HEAOL was analysed at different temperatures, and it was found that there was a two-stage process (Figure 7A). Up to 100 °C, water vaporization occurred, followed by a phase of stable degradation rate. The mass loss increased above 200 °C, which coincided with the temperature at which oleic acid degrades. The increase in the degradation rate observed from 300 °C onwards is likely due to the breaking of the C-C bonds of PIL, which requires higher energy to break these strong covalent bonds [23].

The results of the study showed that the behaviour of the samples of m_1% particles was similar to untreated talc particles (Figure 7B), indicating that the amount of PIL adsorbed/absorbed by the particles in the m-2HEAOL_1%_TC_0.5 formulation was negligible. The total mass loss for m_3% particles was about 0.5% at 500 °C, while for m_8% particles, it was approximately 2%, indicating a greater amount of PIL adsorbed on the particles. The degradation of m-2HEAOL began at around 300 °C, which coincided with

the onset of the acceleration of m-2HEAOL degradation, confirming that this degradation is linked to the PIL molecules adsorbed/absorbed in the talc samples.

It was observed that the gradual mass loss of the particles increased as the amount of m-2HEAOL (m_1%, m_3%, and m_8%) increased. Therefore, higher concentrations of PIL led to a greater amount of this additive interacting with these particles, resulting in prominent peaks associated with the presence of PIL detected in the FTIR analyses (Figure 5E).

3.4.4. Lubrication Mechanism

As shown in previous studies [24,25], PIL m-2HEAOL exhibits lubricating properties when diluted in water. Its ability to adsorb on metal surfaces makes it an effective lubricant [31]. The viscosity of the formulations tested did not affect the lubrication capacity of the lubricants. Therefore, the adsorption capacity of PIL on metal surfaces is even more important in the lubricity of these lubricants in boundary lubrication regimes [47]. Potentially, the adsorption lubrication mechanism, characteristic of PIL, was present even at the lowest concentrations of m-2HEAOL. Therefore, increasing the concentration did not significantly affect the COF in the higher m-2HEAOL concentration.

Unlike the formulations with commercial additives, talc particles did not reduce the COF of formulations containing m-2HEAOL, except for m-2HEAOL_8%_TC_0.5%. The talc-PIL interactions described in item 3.2 had a strong influence on the lubricity of this formulation.

The TGA tests (Figure 7) indicated a greater number of molecules and particles interacting in the 8 wt% PIL formulation, as seen in the identification of peaks associated with PIL in the talc particles through the FTIR analysis (Figure 5). In the XPS analysis (Figure 6), interactions between Si and C and between Mg and O were detected. The Si and C interaction was also detected in the m_3% particle, but it occurred at a lower intensity and had little impact on the lubricity of the formulations in the BUT test. The XPS analysis detected the interaction of Mg and O only in the m_8% particle, which was present in the formulation with the best lubrication performance.

It is known that talc particles have a good lubrication capacity because of their microstructural characteristics. The atoms of the octahedral basal plane, formed by Mg and OH, are weakly linked to the tetrahedral layers of Si and O through Van der Waals bonds. This is why talc has the ability to perfect cleavage in this plane [48]. Then, the settle particles were interposed between the surface of the plate and the pin. Thus, the relative movement between these surfaces during the test can cause the known perfect cleavage of talc and reduce sliding resistance.

According to Schmitzhaus et al. [28], the m-2HEAOL molecule tends to divide in the weakest bond between the oleate ion and the ammonium radical due to the inherent electropositivity of metals. The Mg and O interaction detected using XPS (Figure 6) is likely due to the bond between Mg and the oleate ion, which contains an oxygen atom with a negative charge, favouring this interaction. When the PIL molecule approaches the talc particles, it tends to release the amine radical and form more stable bonds with Mg.

Moreover, the FTIR analysis of the talc particles did not detect the characteristic peak of the NC bond ($1020\text{--}1220\text{ cm}^{-1}$), which is present only in the amine radical of PIL, as shown in Table 1. This reinforces the idea that there was a rupture of the weak Van der Waals bond between the ammonium radical and the oleate ion in the PIL molecule, providing the bond between the Mg ($+\delta$) of talc and the oleate ion ($-\delta$).

The presence of the oleate ion linked to magnesium in the basal plane structure $\{001\}$, as per the proposed mechanism, could potentially enhance the separation of talc particles in this plane. This would increase the lubricity of m_8% particles and the m-2HEAOL_8%_TC_0.5% formulation, ultimately leading to a decrease in the COF value. Figure 8 graphically illustrates this mechanism.

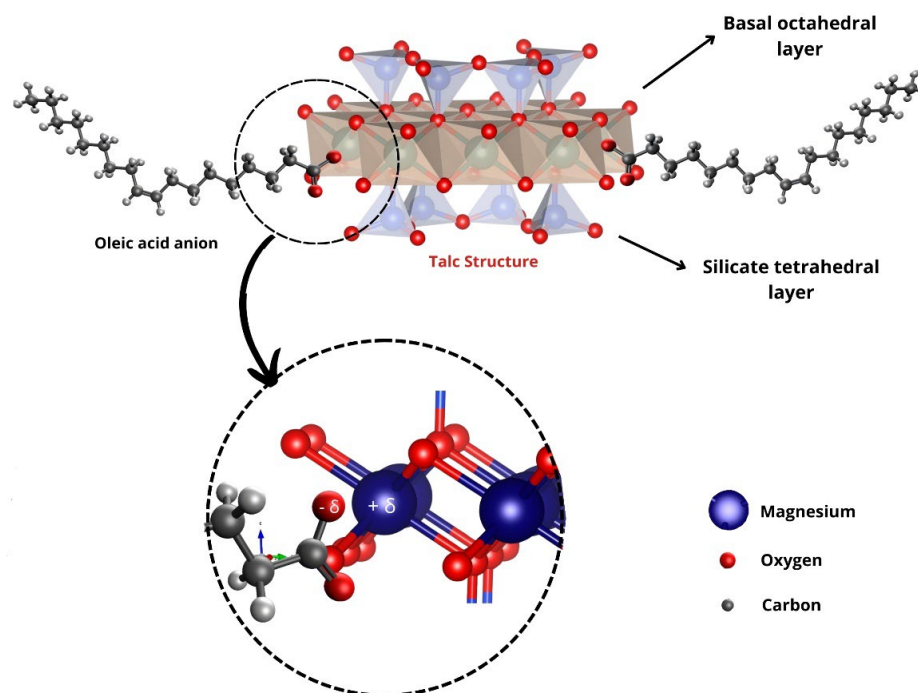


Figure 8. Schematic representation of the interaction between Mg present in the basal layer of talc and O⁻ present in the oleate ion of m-2HEAOL.

4. Conclusions

The synergic effect of talc particles and PILs in water-based lubricants was investigated. The tests aimed to evaluate the tribological performance of these formulations in bending under tension tests, which simulate deep drawing operations. The main results are presented below.

- The tests that did not include additional particles demonstrated that m-2HEAOL has comparable lubricating potential to that of commercial additives in water-based lubricants for stamping operations.
- In the m-2HEAOL_1%_TC_0.5% and m-2HEAOL_3%_TC_0.5% formulations, the addition of talc particles did not notably contribute to COF reduction. Therefore, the lubrication effectiveness of the PIL was more powerful than the influence of the talc.
- It was discovered that m-2HEAOL can interact with talc particles. When the concentration of PIL is higher, as in the case of the m-2HEAOL_8%_TC_0.5% formulation, this interaction becomes more noticeable, affecting the COF value. The PIL oleate molecules bind with the Mg in the basal layer of talc, which increases the mineral's cleavage capacity. This results in an improvement in the lubricity of the formulation.

The results show that the combination of 8 wt% concentrations of m-2HEAOL and talc is beneficial for BUT tests, indicating that this particle has the potential to replace graphite in water-based formulations.

Author Contributions: V.V.d.C.: Conceptualization methodology; validation, formal analysis, investigation, writing—review and editing; project administration. C.E.: Data curation, formal analysis, writing—review and editing. M.B.: formal analysis, writing—review and editing. L.C.N.: Conceptualization methodology; validation, formal analysis. L.E.: formal analysis, writing—review and editing. L.M.d.S.: data curation; review and editing; R.M.V.: data curation; review and editing; S.M.: supervision, review and editing. R.M.S.: supervision, review and editing, data curation. C.d.F.M.: supervision, review and editing, data curation, project administration. All authors have read and agreed to the published version of the manuscript.

Funding: This research was funded by CAPES grant number: PROEX 88881.844968/2023-01); Research Support Foundation of Rio Grande do Sul (FAPERGS), grant number 22/2551-0001071-7); National Council for Scientific and Technological Development CNPq, grant numbers: 350561/2023-0, 313493/2023-5 and 311342/2022-1.

Data Availability Statement: The raw data supporting the conclusions of this article will be made available by the authors on request.

Conflicts of Interest: The authors declare no conflicts of interest.

References

1. Trzepieciński, T.; Lemu, H.G. Effect of Lubrication on Friction in Bending under Tension Test-Experimental and Numerical Approach. *Metals* **2020**, *10*, 544. [[CrossRef](#)]
2. Pereira, M.P.; Yan, W.; Rolfe, B.F. Contact Pressure Evolution and Its Relation to Wear in Sheet Metal Forming. *Wear* **2008**, *265*, 1687–1699. [[CrossRef](#)]
3. Trzepieciński, T.; Fejkiel, R. On the Influence of Deformation of Deep Drawing Quality Steel Sheet on Surface Topography and Friction. *Tribol. Int.* **2017**, *115*, 78–88. [[CrossRef](#)]
4. Luiz, V.D.; Santos, A.J.d.; Câmara, M.A.; Rodrigues, P.C.d.M. Influence of Different Contact Conditions on Friction Properties of AISI 430 Steel Sheet with Deep Drawing Quality. *Coatings* **2023**, *13*, 771. [[CrossRef](#)]
5. Andreasen, J.L.; Olsson, D.D.; Chodnikiewicz, K.; Bay, N. Bending Under Tension Test with Direct Friction Measurement. *Proc. Inst. Mech. Eng. Part B J. Eng. Manuf.* **2006**, *220*, 73–80. [[CrossRef](#)]
6. Moghadam, M.; Suleiman, M.H.; Christiansen, P.; Bay, N. Acoustic Emission Monitoring of the Bending under Tension Test. *Procedia Eng.* **2017**, *207*, 1421–1426. [[CrossRef](#)]
7. Ceron, E.; Martins, P.A.F.; Bay, N. Thermal Analysis of Bending under Tension Test. *Procedia Eng.* **2014**, *81*, 1805–1810. [[CrossRef](#)]
8. Folle, L.; Schaeffer, L. New Proposal to Calculate the Friction in Sheet Metal Forming through Bending under Tension Test. *Mater. Res.* **2019**, *22*, e20190523. [[CrossRef](#)]
9. Song, H.-J.; Li, N. Frictional Behavior of Oxide Graphene Nanosheets as Water-Base Lubricant Additive. *Appl. Phys. A* **2011**, *105*, 827–832. [[CrossRef](#)]
10. Rojas-Campanur, M.; Lara-Romero, J.; Chiñas-Castillo, F.; Alonso-Nuñez, G. Tribological Performance of Rosin Acid Additives in Water Based Lubricants. *Tribol. Online* **2007**, *2*, 29–33. [[CrossRef](#)]
11. Polajnar, M.; Čoga, L.; Kalin, M. Base Lubricants for Green Stamping: The Effects of Their Structure and Viscosity on Tribological Performance. *Friction* **2023**, *11*, 1741–1754. [[CrossRef](#)]
12. Aiman, Y.; Syahrullail, S.; Kameil, A.H. Tribological in Metal Forming Process and the Use of Bio Lubricant as Metal Forming Lubricant: A Review. *J. Teknol.* **2024**, *86*, 95–114. [[CrossRef](#)]
13. García-Miranda, J.S.; Aguilera-Camacho, L.D.; Hernández-Sierra, M.T.; Moreno, K.J. A Comparative Analysis of the Lubricating Performance of an Eco-Friendly Lubricant vs Mineral Oil in a Metallic System. *Coatings* **2023**, *13*, 1314. [[CrossRef](#)]
14. Trzepieciński, T. Tribological Performance of Environmentally Friendly Bio-Degradable Lubricants Based on a Combination of Boric Acid and Bio-Based Oils. *Materials* **2020**, *13*, 3892. [[CrossRef](#)] [[PubMed](#)]
15. Rahman, M.H.; Warneke, H.; Webbert, H.; Rodriguez, J.; Austin, E.; Tokunaga, K.; Rajak, D.K.; Menezes, P.L. Water-Based Lubricants: Development, Properties, and Performances. *Lubricants* **2021**, *9*, 73. [[CrossRef](#)]
16. Greaves, T.L.; Drummond, C.J. Protic Ionic Liquids: Properties and Applications. *Chem. Rev.* **2008**, *108*, 206–237. [[CrossRef](#)] [[PubMed](#)]
17. Avilés, M.-D.; Pamies, R.; Sanes, J.; Carrión, F.-J.; Bermúdez, M.-D. Fatty Acid-Derived Ionic Liquid Lubricant. Protic Ionic Liquid Crystals as Protic Ionic Liquid Additives. *Coatings* **2019**, *9*, 710. [[CrossRef](#)]
18. Avilés, M.D.; Carrión-Vilches, F.J.; Sanes, J.; Bermúdez, M.D. Diprotic Ammonium Succinate Ionic Liquid in Thin Film Aqueous Lubrication and in Graphene Nanolubricant. *Tribol. Lett.* **2019**, *67*, 26. [[CrossRef](#)]
19. Espinosa, T.; Sanes, J.; Jiménez, A.-E.; Bermúdez, M.-D. Protic Ammonium Carboxylate Ionic Liquid Lubricants of OFHC Copper. *Wear* **2013**, *303*, 495–509. [[CrossRef](#)]
20. Gusain, R.; Dhingra, S.; Khatri, O.P. Fatty-Acid-Constituted Halogen-Free Ionic Liquids as Renewable, Environmentally Friendly, and High-Performance Lubricant Additives. *Ind. Eng. Chem. Res.* **2016**, *55*, 856–865. [[CrossRef](#)]
21. Pamies, R.; Avilés, M.D.; Arias-Pardilla, J.; Carrión, F.J.; Sanes, J.; Bermúdez, M.D. Rheological Study of New Dispersions of Carbon Nanotubes in the Ionic Liquid 1-Ethyl-3-Methylimidazolium Dicyanamide. *J. Mol. Liq.* **2019**, *278*, 368–375. [[CrossRef](#)]
22. Saurín, N.; Avilés, M.D.; Espinosa, T.; Sanes, J.; Carrión, F.J.; Bermúdez, M.D.; Iglesias, P. Carbon Nanophases in Ordered Nanofluid Lubricants. *Wear* **2017**, *376–377*, 747–755. [[CrossRef](#)]
23. Ortega Vega, M.R.; Ercolani, J.; Mattedi, S.; Aguzzoli, C.; Ferreira, C.A.; Rocha, A.S.; Malfatti, C.F. Oleate-Based Protic Ionic Liquids as Lubricants for Aluminum 1100. *Ind. Eng. Chem. Res.* **2018**, *57*, 12386–12396. [[CrossRef](#)]
24. de Castro, V.V.; dos Santos, L.M.; Antonini, L.M.; Schroeder, R.M.; Mattedi, S.; Souza, K.S.; Pereira, M.B.; Einloft, S.; dos Santos, C.A.; de Fraga Malfatti, C. Water-Based Lubricant Containing Protic Ionic Liquids and Talc Lubricant Particles: Wear and Corrosion Analysis. *Wear* **2023**, *518–519*, 204633. [[CrossRef](#)]

25. de Castro, V.V.; dos Santos, L.M.; Antonini, L.M.; Schroeder, R.M.; Mattedi, S.; Souza, K.S.; Pereira, M.B.; de Lima Lessa, C.R.; Einloft, S.; dos Santos, C.A.; et al. A Tribological and Electrochemical Study of Protic Ionic Liquid and Bentonite Particles Used as Lubricating Additives in Water-Based Lubricants. *J. Bio-Tribo-Corros.* **2023**, *9*, 51. [[CrossRef](#)]
26. Schmitzhaus, T.E.; Vega, M.R.O.; Schroeder, R.; Muller, I.L.; Mattedi, S.; Taryba, M.; Fernandes, J.C.S.; de Fraga Malfatti, C. Localized Corrosion Behavior Studies by SVET of 1010 Steel in Different Concentrations of Sodium Chloride Containing [Im-2HEA][O] Ionic Liquid as Corrosion Inhibitor. *Electrochim. Acta* **2022**, *419*, 140385. [[CrossRef](#)]
27. Schmitzhaus, T.E.; Ortega Vega, M.R.; Schroeder, R.; Muller, I.L.; Mattedi, S.; Malfatti, C.d.F. N-Methyl-2-Hydroxyethylammonium Oleate Ionic Liquid Performance as Corrosion Inhibitor for Mild Steel in Hydrochloric Acid Medium. *Mater. Corros.* **2020**, *71*, 1885–1902. [[CrossRef](#)]
28. Schmitzhaus, T.E.; Ortega Vega, M.R.; Schroeder, R.; Muller, I.L.; Mattedi, S.; Malfatti, C.d.F. An Amino-based Protic Ionic Liquid as a Corrosion Inhibitor of Mild Steel in Aqueous Chloride Solutions. *Mater. Corros.* **2020**, *71*, 1175–1193. [[CrossRef](#)]
29. Ortega Vega, M.R.; Baldin, E.K.; Pereira, D.P.; Martins, M.C.S.; Pranke, P.; Horn, F.; Pinheiro, I.; Vieira, A.; Espiña, B.; Mattedi, S.; et al. Toxicity of Oleate-Based Amino Protic Ionic Liquids towards *Escherichia coli*, Danio Rerio Embryos and Human Skin Cells. *J. Hazard. Mater.* **2022**, *422*, 126896. [[CrossRef](#)]
30. Rudenko, P.; Bandyopadhyay, A. Talc as Friction Reducing Additive to Lubricating Oil. *Appl. Surf. Sci.* **2013**, *276*, 383–389. [[CrossRef](#)]
31. Tang, Z.; Li, S. A Review of Recent Developments of Friction Modifiers for Liquid Lubricants (2007–Present). *Curr. Opin. Solid State Mater. Sci.* **2014**, *18*, 119–139. [[CrossRef](#)]
32. Jha, A.K.; Dan, T.K.; Prasad, S.V.; Rohatgi, P.K. Aluminium Alloy-Solid Lubricant Talc Particle Composites. *J. Mater. Sci.* **1986**, *21*, 3681–3685. [[CrossRef](#)]
33. Akbulut, M. Nanoparticle-Based Lubrication Systems. *J. Powder Metall. Min.* **2012**, *1*, e01. [[CrossRef](#)]
34. Wada, S.; Hayashi, H. Hydrodynamic Lubrication of Journal Bearings by Pseudo-Plastic Lubricants: Part 2, Experimental Studies. *Bull. JSME* **1971**, *14*, 279–286. [[CrossRef](#)]
35. Nascimento, R.C.a.M.; Amorim, L.V.; Santana, L.N.L. Desenvolvimento de fluidos aquosos com bentonita para perfuração de poços de petróleo onshore. *Cerâmica* **2010**, *56*, 179–187. [[CrossRef](#)]
36. Felder, E.; Levrau, C. Analysis of the Lubrication by a Pseudoplastic Fluid: Application to Wire Drawing. *Tribol. Int.* **2011**, *44*, 845–849. [[CrossRef](#)]
37. Arif, M.; Kango, S.; Shukla, D.K. Analysis of Textured Journal Bearing with Slip Boundary Condition and Pseudoplastic Lubricants. *Int. J. Mech. Sci.* **2022**, *228*, 107458. [[CrossRef](#)]
38. Mierczynska-Vasilev, A.; Ralston, J.; Beattie, D.A. Adsorption of Modified Dextrins on Talc: Effect of Surface Coverage and Hydration Water on Hydrophobicity Reduction. *Langmuir* **2008**, *24*, 6121–6127. [[CrossRef](#)] [[PubMed](#)]
39. Casanova, H.; Orrego, J.A.; Zapata, J. Oil Absorption of Talc Minerals and Dispersant Demand of Talc Mineral Non-Aqueous Dispersions as a Function of Talc Content: A Surface Chemistry Approach. *Colloids Surf. A Physicochem. Eng. Asp.* **2007**, *299*, 38–44. [[CrossRef](#)]
40. da Silva Bullmann, M.; de Castro, V.V.; Coutinho, D.A.K.; Lopes, F.C.; Maurmann, N.; Pereira, M.B.; Rodrigues, M.; Pranke, P.; Ferraz, M.P.; Lopes, M.A.; et al. Eucalyptus Globulus Essential Oil Thin Film Polymerized by Cold Plasma on Ti6Al4V: Sterilization Effect, Antibacterial Activity, Adhesion, and Viability of Mesenchymal Stem Cells. *Plasma Process. Polym.* **2023**, *20*, e2300075. [[CrossRef](#)]
41. Derkowski, A.; Rodo, J.; McCarty, D. Cation Exchange Capacity and Water Content of Opal in Sedimentary Basins: Example from the Monterey Formation, California. *Am. Mineral.* **2015**, *100*, 1244–1256. [[CrossRef](#)]
42. Mai, Q.; Zhou, H.; Ou, L. Flotation Separation of Chalcopyrite and Talc Using Calcium Ions and Calcium Lignosulfonate as a Combined Depressant. *Metals* **2021**, *11*, 651. [[CrossRef](#)]
43. Zhang, Y.; Zhu, L.; Chen, L.; Liu, L.; Ye, G. Influence of Magnesia on Demoulding Strength of Colloidal Silica-Bonded Castables. *Rev. Adv. Mater. Sci.* **2019**, *58*, 32–37. [[CrossRef](#)]
44. Kaur, A.; Chahal, P.; Hogan, T. Selective Fabrication of SiC/Si Diodes by Excimer Laser under Ambient Conditions. *IEEE Electron. Device Lett.* **2016**, *37*, 142–145. [[CrossRef](#)]
45. Corneille, J.S.; He, J.-W.; Goodman, D.W. XPS Characterization of Ultra-Thin MgO Films on a Mo(100) Surface. *Surf. Sci.* **1994**, *306*, 269–278. [[CrossRef](#)]
46. Hazwani Dzulkafli, H.; Ahmad, F.; Ullah, S.; Hussain, P.; Mamat, O.; Megat-Yusoff, P.S.M. Effects of Talc on Fire Retarding, Thermal Degradation and Water Resistance of Intumescent Coating. *Appl. Clay Sci.* **2017**, *146*, 350–361. [[CrossRef](#)]
47. Hsu, S.M.; Gates, R.S. Boundary Lubricating Films: Formation and Lubrication Mechanism. *Tribol. Int.* **2005**, *38*, 305–312. [[CrossRef](#)]
48. Prasad, B.K.; Rathod, S.; Modi, O.P.; Yadav, M.S. Influence of Talc Concentration in Oil Lubricant on the Wear Response of a Bronze Journal Bearing. *Wear* **2010**, *269*, 498–505. [[CrossRef](#)]

Disclaimer/Publisher’s Note: The statements, opinions and data contained in all publications are solely those of the individual author(s) and contributor(s) and not of MDPI and/or the editor(s). MDPI and/or the editor(s) disclaim responsibility for any injury to people or property resulting from any ideas, methods, instructions or products referred to in the content.